Leveraging Anatomical Constraints for Pneumothorax Segmentation

Han Yuan[1], Chuan Hong[2], Nguyen Tuan Anh Tran[3], Xinxing Xu[4], Nan Liu[1,5]

[1]Duke-NUS Medical School [2]Duke University [3]Singapore General Hospital [4]A*STAR [5]SingHealth AI Office

Introduction

Pneumothorax is a critical thoracic condition resulting from the abnormal accumulation of air in the **pleural space** between the lungs and chest wall. On 2D chest radiographs, pneumothorax occurs within the thoracic cavity and outside of the mediastinum and we refer to this area as "**lung+ space**".

Deep learning (DL) has increasingly been utilized to segment pneumothorax lesions from radiographs in an end-to-end approach and neglects that pneumothorax is inherently location-sensitive.

Model Overview

The proposed pipeline contains **three indispensable phases** to obtain sample-specific lung+ space, select well-behaved lung+ space, and implement constrained training of pneumothorax segmenter.

Figure 1: Diagram of the proposed method

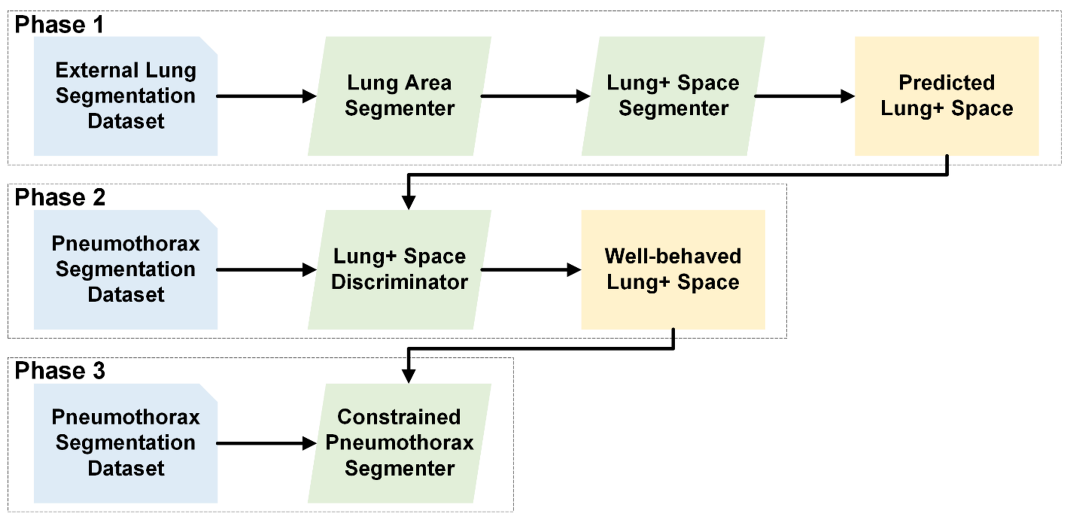

Phase 1: Constraint Generation

In Phase 1, we develop an **auxiliary lung segmenter** using public lung segmentation datasets. Then it is integrated with **morphological operations**, including connected component cutoff, closing, and dilation to derive a lung+ space segmenter.

This refined segmenter is subsequently deployed on the target dataset of pneumothorax segmentation to predict lung+ space.

Figure 2: Pipeline of the constraint generation

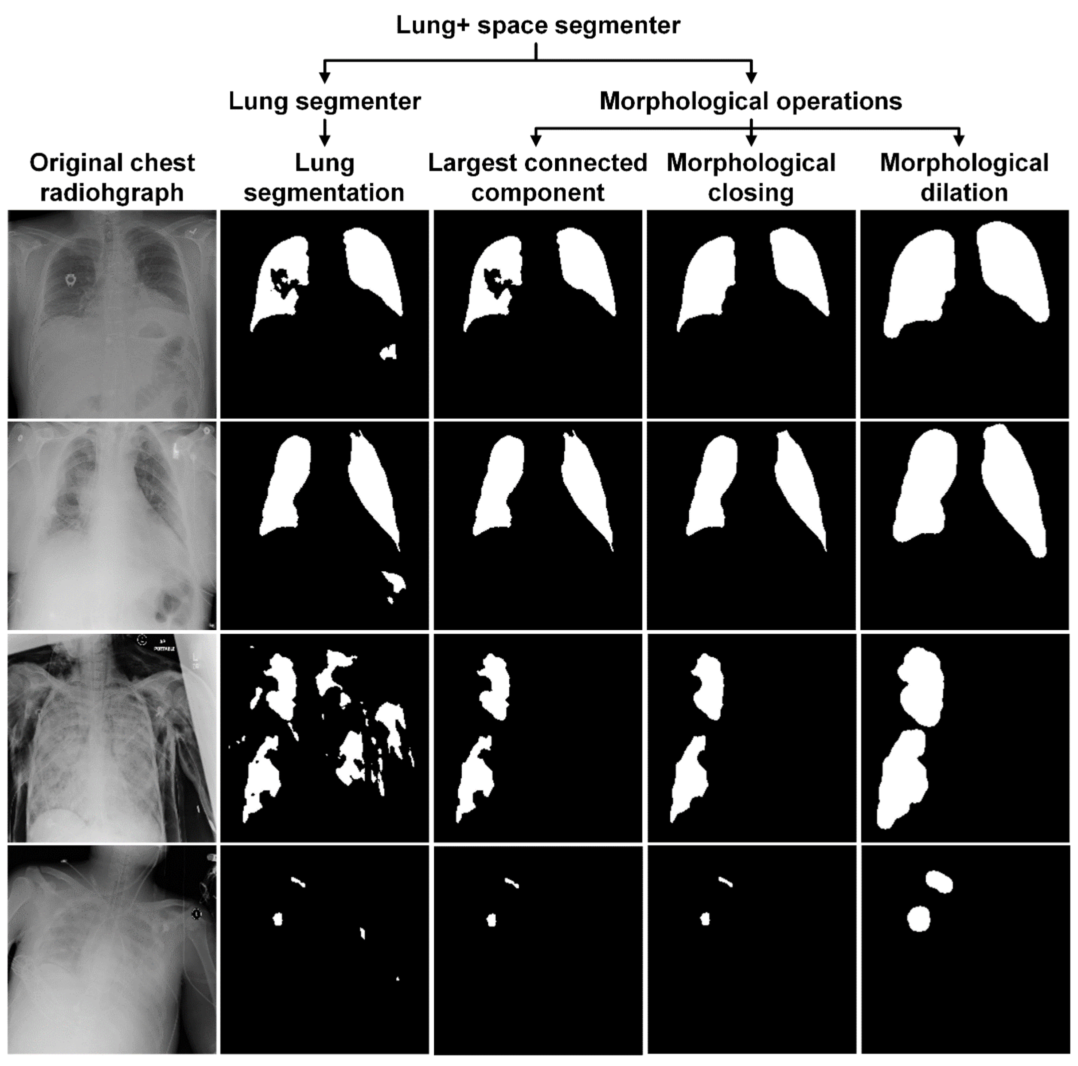

Phase 2: Constraint Selection

In Phase 2, we introduce a **lung+ space discriminator**, crafted using the training and validation dataset for the pneumothorax segmentation, filtering out inaccurately predicted lung+ spaces from Phase 1, ensuring only **high-quality constraints** are retained.

Phase 3: Constrained Training

In Phase 3, with the selected lung+ space from Phase 2, we proceed to **train** the pneumothorax segmenter using a **constrained approach**.

Specifically, in a typical training stage of a single disease segmenter, we consider a dataset D consisting of N input images I_i and their respective lesion segmentations S_i. Model Y is trained by minimizing the overall loss L averaging sample-wise loss l such as Dice or cross-entropy between the model output $Y(I_i)$ and the ground-truth mask S_i.

$$l(Y(I_i), S_i)$$

Here the disease occurrence area is introduced as a **penalty** in the loss function to guide the model's focus on the disease occurrence area.

Specifically, the loss function will be supplemented with a novel penalty term P comparing the model output $Y(I_i)$ with a sample-specific constraint C_i:

$$l(Y(I_i), S_i) + \lambda * P(Y(I_i), C_i)$$

λ is a positive hyper-parameter, and $P(Y(I_i), C_i)$ denotes the proposed penalty term:

$$1 - |Y(I_i) \bigcap C_i| / |Y(I_i)|$$

Implementation Details

We implemented the experiments on a Dell Precision 7920 Workstation with an Intel Xeon Silver 4210 CPU and an NVIDIA GeForce RTX 2080 Super GPU.

Table 1: Default experimental details

Phase	Hyper-parameter	Candidate
1	Architecture	U-Net
	Backbone	VGG-11
	Loss function	Dice loss
	Optimizer	SGD
2	Backbone	VGG-11
	Loss function	Cross entropy
	Optimizer	SGD
3	Architecture	U-Net, LinkNet, PSPNet
	Backbone	VGG-11
	Loss function	Dice loss
	Optimizer	SGD

Quantitative Results

We quantitatively compared the constrained and the baseline segmentation performance across different combinations of architectures and backbones. The constrained version **consistently outperformed** the baseline method.

Table 2: Internal segmenter evaluation

Architectures	Methods	IoU	DSC
	Baseline	0.316	0.441
U-Net	Ours	0.336	0.461
	Improvement	**6.3%**	**4.5%**
	Baseline	0.305	0.426
LinkNet	Ours	0.322	0.447
	Improvement	**5.6%**	**4.9%**
	Baseline	0.302	0.424
PSPNet	Ours	0.307	0.429
	Improvement	**1.7%**	**1.2%**

To evaluate the generalization ability, we further deployed the constrained and the baseline segmenter on an external dataset without fine-tuning.

Table 3: External segmenter evaluation

Architectures	Methods	IoU	DSC
	Baseline	0.269	0.384
U-Net	Ours	0.298	0.416
	Improvement	**10.8%**	**8.3%**
	Baseline	0.270	0.386
LinkNet	Ours	0.270	0.382
	Improvement	**0.0%**	**-1.0%**
	Baseline	0.245	0.355
PSPNet	Ours	0.262	0.376
	Improvement	**6.9%**	**5.9%**

Qualitative Results

We provided a comparative visualization of pneumothorax segmentation between the constrained and baseline segmenters using the architecture of U-Net and the backbone of VGG-11.

Figure 3: Comparative examples

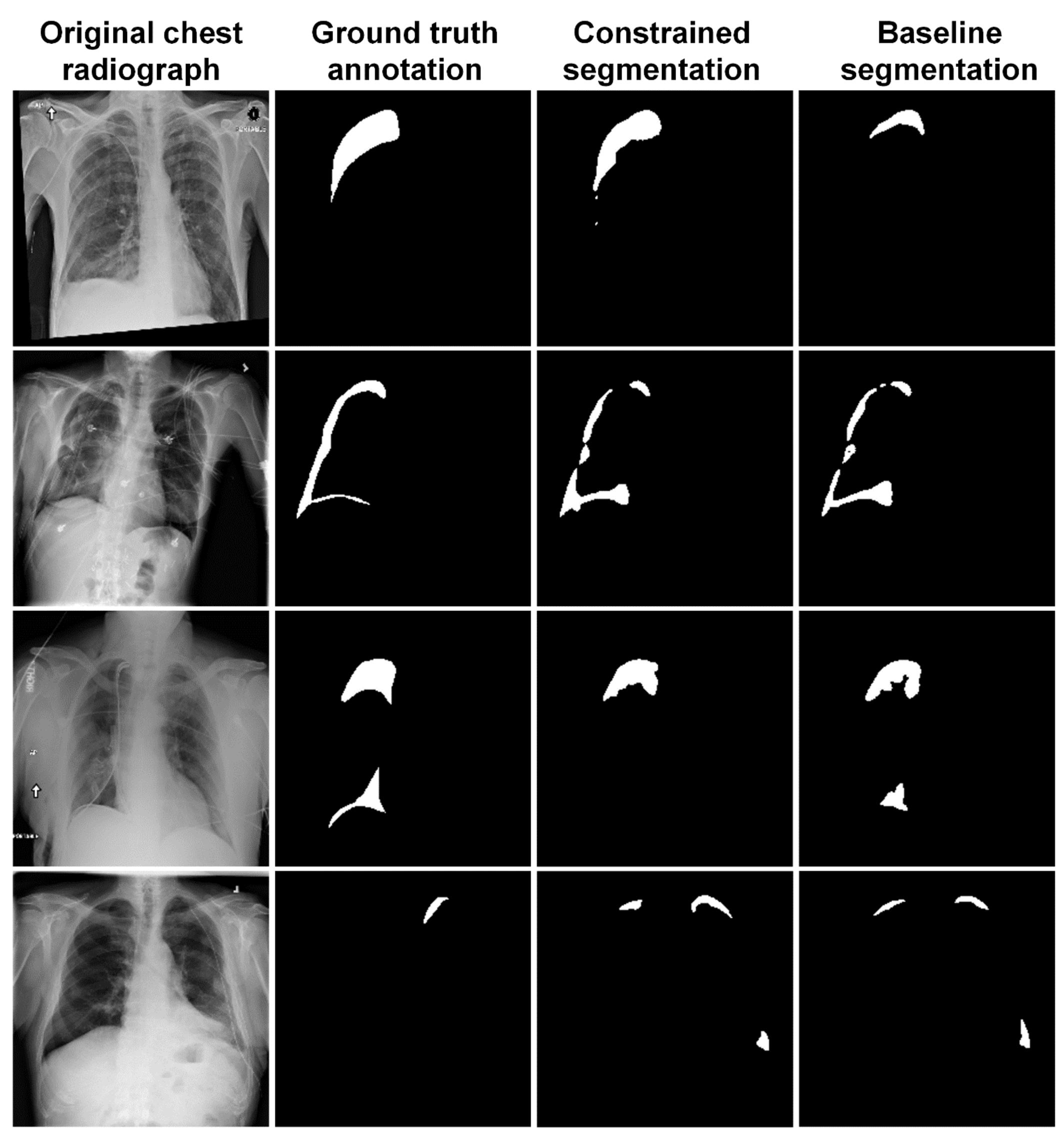

References

[1] Jonathan B Imran and Alexander L Eastman. Pneumothorax. *Journal of the American Medical Association*, 2017.
[2] Michael H Baumann and Marc Noppen. Pneumothorax. *Respirology*, 2004.
[3] Steven A Sahn and John E Heffner. Spontaneous pneumothorax. *New England Journal of Medicine*, 2000.
[4] Erdi Çallı, Ecem Sogancioglu, van Ginneken, et al. Deep learning for chest x-ray analysis: A survey. *Medical Image Analysis*, 2021.
[5] Adriel Saporta, Xiaotong Gui, Ashwin Agrawal, et al. Benchmarking saliency methods for chest x-ray interpretation. *Nature Machine Intelligence*, 2022.
[6] Hong-Gyu Jung, Woo-Jeoung Nam, Hyun-Woo Kim, et al. Weakly supervised thoracic disease localization via disease masks. *Neurocomputing*, 2023.
[7] Mathilde Bateson, Hoel Kervadec, Jose Dolz, et al. Source-free domain adaptation for image segmentation. *Medical Image Analysis*, 2022.
[8] Hoel Kervadec, Jose Dolz, Meng Tang, et al. Constrained-cnn losses for weakly supervised segmentation. *Medical Image Analysis*, 2019.
[9] Mathilde Bateson, José Dolz, Hoel Kervadec, et al. Constrained domain adaptation for image segmentation. *IEEE Transactions on Medical Imaging*, 2021.

DukeNUS Medical School